A Survey of Possible Passive Antenna Applications of High-Temperature Superconductors

Robert J. Dinger, *Member, IEEE*, Donald R. Bowling, and Anna M. Martin

(*Invited Paper*)

***Abstract*—A survey of possible applications of high-temperature superconductors (HTS's) to antennas and antenna feed networks is presented. The frequency range of consideration is 1 MHz to 100 GHz. Three antenna application areas seem appropriate for HTS material: electrically small antennas and their matching networks; feed and matching networks for compact arrays with enhanced directive gain (superdirective arrays); and feed networks for millimeter-wave arrays. Preliminary experimental results are presented on YBaCuO and TlBaCaCuO 500 MHz half-loop antennas that show an increase in radiation efficiency (compared with a copper antenna at the same temperature) by a factor of 5 for the HTS antennas.**

***Keywords*—High temperature superconductivity; antennas; electrically small antennas; antenna feed networks; antenna arrays; superdirectivity**

I. Introduction

In this paper we examine the potential of high-temperature superconductors (HTS's) for antenna system applications. The reduced surface resistance, R_s, of high-temperature superconductors has the potential to lower the insertion loss of RF and microwave devices by many dB's. The loss suffered between the transmission line input/output port and the radiation "ports" of an antenna system can be substantial, and HTS components can lead to a performance enhancement that justifies the cost and complication of cooling.

Our primary frequency range of interest is about 1 MHz to 100 GHz. Although the antennas that have been developed from low-temperature superconductors have operated at frequencies substantially below this range in the 3 to 300 Hz frequency band [1], these antennas are most properly viewed as a type of magnetometer. They rely on the very low noise properties of Josephson junctions, which have yet to be demonstrated reliably in HTS material. Our focus is on the passive components in antenna systems. Active components, such as variable phase shifters, attenuators, and receivers integrated with the antenna, that exploit HTS material await further development before their application to antenna systems can be reasonably examined.

Below, we discuss in some detail three application areas: electrically short antennas and their matching networks; feed networks and elements for superdirective antenna arrays; and millimeter-wave array feed networks. In part to demonstrate the enhancement in radiation efficiency possible, we present results on two half-loop HTS antennas operated at 500 MHz. We then mention the possibility of integrated passive feed networks of components that provide signal processing in the spatial, temporal, and frequency domains. We end with a brief discussion of practical considerations. This paper is one in a lengthening series of papers examining the potential antenna applications of HTS's [2]–[4].

Manuscript received December 18, 1990; revised April 30, 1991. This work was supported by the Office of Naval Research and the Defense Advanced Research Projects Agency.

The authors are with the RF and Microwave Technology Branch, Naval Weapons Center, China Lake, CA 93555.

IEEE Log Number 9101404.

II. Electrically Short Antennas

A. Antenna Efficiency

Fig. 1 is the equivalent circuit of an antenna connected to a load. The resistance R_d accounts for conductor and dielectric losses in both the antenna and the matching circuit. When conjugately matched for maximum power transfer such that $X_L = -X_a$ and $R_L = R_r + R_d$, the radiation efficiency is given by

$$\eta = \text{radiated power/input power} = P_r/P_{\text{in}} = R_r/(R_r + R_d). \quad (1)$$

The input power is calculated at the input to the matching network, rather than the antenna terminals.

Because HTS material reduces the conductor losses in R_d, the antennas that benefit from HTS materials are those for which $R_d \geq R_r$. The only class of antennas for which this is generally true are electrically small antennas, i.e., antennas with dimensions that are small compared with the wavelength of operation. Resonant and aperture antennas usually have $R_r \gg R_d$.

The bandwidth of the conjugately matched antenna with center frequency ω_0 is given by

$$B = \omega_0 R_L / X_a = \omega_0 R_r / X_a + \omega_0 R_d / X_a. \quad (2)$$

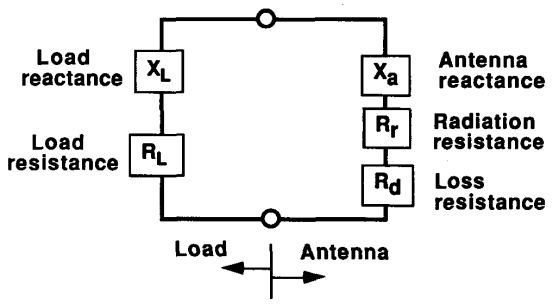

Fig. 1. Equivalent circuit of an antenna connected to a load.

The quantity $B_r = \omega_0 R_r / X_a$ is the *radiation bandwidth*, which is the "intrinsic" bandwidth established by the configuration of the antenna and which is independent of the material from which the antenna is made. A feature of electrically small antennas is that X_a is large and R_r small, so that the radiation bandwidth is narrow. Combining the definition of B_r with (1) and (2) yields

$$\eta B = B_r. \tag{3}$$

Hence, the product of the efficiency and the overall antenna bandwidth is a constant. Clearly, any increase in efficiency brought about by using HTS material will produce a narrowing of bandwidth. The radiation bandwidth can often be increased for a given size antenna by such techniques as the top loading of monopoles [5], but there is a fundamental limit to B_r established by the size of the antenna [6].

B. Example: A Short Dipole Antenna and Matching Network

To assess the potential improvement in efficiency that is possible by replacing the normal conductors with HTS's, we have analyzed in detail the electrically small antenna shown in Fig. 2. A short dipole of overall length L is driven from a balanced twin-lead transmission line. A shunt short-circuit stub is used to match the impedance of the transmission line to the antenna. The twin-lead transmission line is enclosed in a dielectric, which is required in a practical application both for support and efficient cooling of the conductors. The transmission line parameters were selected to give a practical size in the 100 MHz to 1 GHz frequency range and to produce a 50 Ω impedance with a reasonable value of dielectric constant.

The antenna and the matching network in Fig. 2 are probably a feasible configuration for a practical HTS antenna; indeed, it is similar to the HTS antenna for which measurements were presented in [7]. However, this configuration also serves as a surrogate for a wide variety of electrically short antennas, such as a wire monopole driven by coax line and a printed circuit dipole driven by a microstrip transmission line.

We have discussed this calculation in [8]; here, we summarize the results. In Fig. 3 we plot the efficiency as a function of the surface resistance for a dipole length of

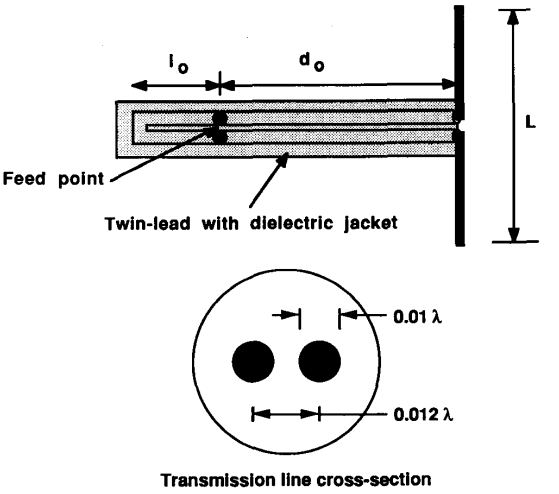

Fig. 2. Dipole antenna with single-stub matching network. The dielectric constant of the jacket is $\epsilon' = 3.58\epsilon_0$.

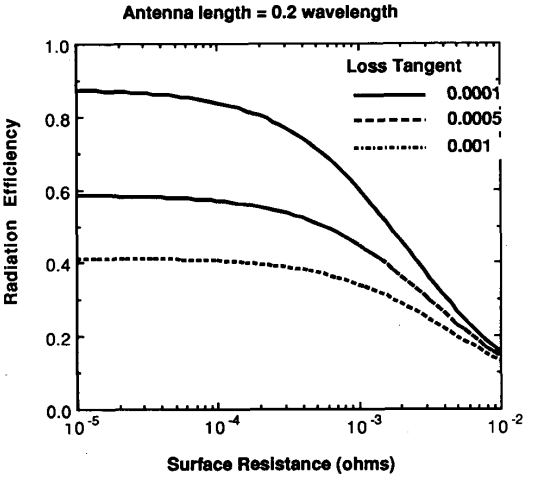

Fig. 3. Radiation efficiency for the dipole and antenna and matching network of Fig. 2 for three dielectric loss tangents.

0.2λ, with the dielectric loss tangent as a parameter. The three-decade range of R_s shown encompasses the surface resistance values that can reasonably be expected from improved HTS material. As R_s is lowered, the efficiency improves as expected, but it levels off at the value of R_s where dielectric losses begin to dominate. This value occurs when the dielectric attenuation constant, α_d, begins to exceed the conductor attenuation constant, α_c. Unless the loss tangent is 10^{-4} or less, only a rather modest improvement in radiation efficiency can be realized.

Fig. 4 is a plot of radiation efficiency as a function of dipole length. A radiation efficiency approaching 100% appears to be possible with a dipole as short as 0.1λ. The bandwidth–efficiency trade-off of (3) is demonstrated in

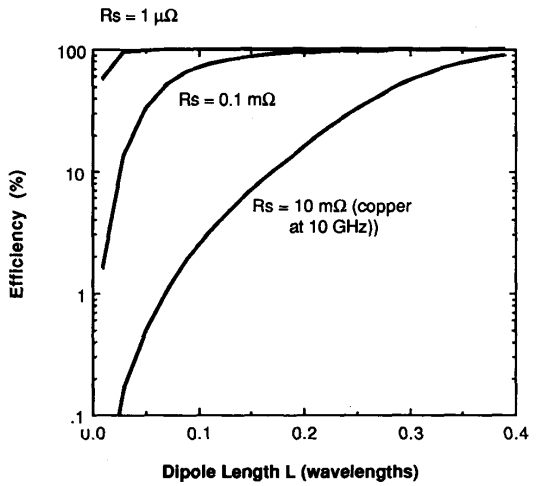

Fig. 4. Efficiency versus dipole length.

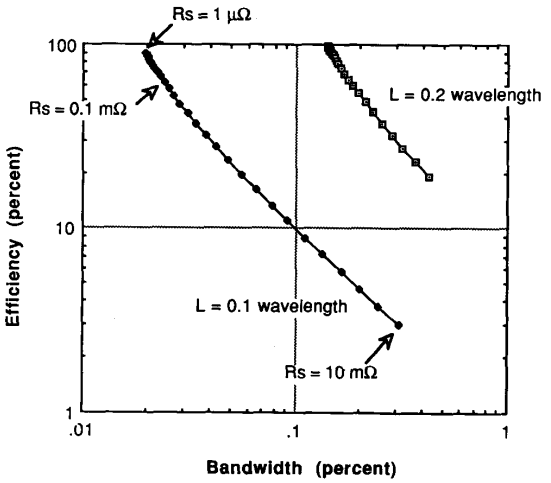

Fig. 5. Efficiency versus bandwidth. Each curve is generated by varying R_s over four decades; the R_s at three selected points is shown on the $L = 0.1\lambda$ curve. The relative locations of these three points fall at similar points on the $L = 0.2\lambda$ curve.

Fig. 5. The curves for the two dipole lengths are traced out by varying the surface resistance as indicated. Clearly, the price for high efficiency is narrow bandwidth.

Low-loss materials in the transmission line between the matching stub and the antenna are especially critical. In Fig. 6 we plot the fractional power losses in the various portions of the antenna and matching network for a representative R_s and loss tangent. The large standing waves between the stub and antenna terminals produce most of the loss; the antenna ohmic losses actually account for the smallest fraction of the losses in this example. Fig. 6 also suggests that only the matching network needs to be made from HTS material.

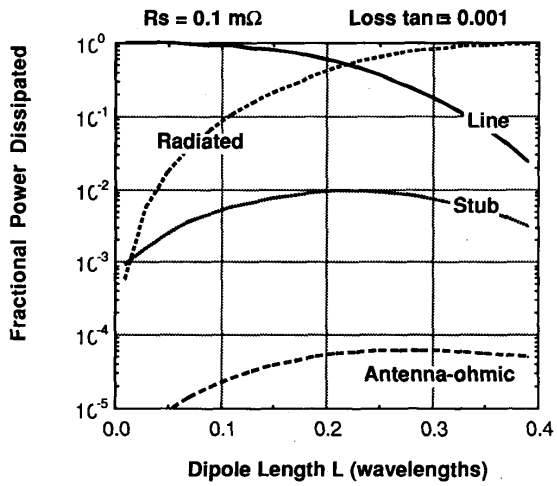

Fig. 6. The fraction of power dissipated in the indicated portions of the antenna and matching network. The portion labeled "line" refers to the section of transmission line between the stub and the antenna.

C. Experimental Results: A Half-Loop Antenna

Preliminary measurements have been taken at 500 MHz on two antennas with the design shown in Fig. 7. The antennas have an HTS film patterned on a $LaAlO_3$ substrate to form a half-loop over a ground plane. The half-loop on the top half of the substrate protrudes through a slot in a copper ground plane. The coupled-line section is a matching network that transforms the input impedance of the antenna ($Z_{in} = 0.1 + j80\ \Omega$) to the 50 Ω impedance of the feed line.

Two different versions of the antenna have been measured to date. One antenna is fabricated from YBaCuO, with its matching network ground plane fabricated from another film of YBaCuO positioned behind the antenna substrate in a sandwich structure. The second antenna is fabricated from TlBaCaCuO; its matching network ground plane is also TlBaCaCuO on the same substrate as the antenna circuit. The antennas are mounted under an evacuated hemispherical Teflon radome and cooled by a closed-cycle refrigerator.

The first experimental measurements of the radiation efficiency of these antenna are shown in Fig. 8. For comparison, the efficiency of a copper antenna and matching network of the same design and formed on the same substrate material is also shown. Below the superconducting transition temperature, the YBaCuO antenna achieves an efficiency of about 16% and the TlBaCaCuO 37%, compared with 7% for the copper antenna. The bandwidths are 4.0 MHz and 1.0 MHz, respectively. Non-HTS losses in the substrate and the copper antenna ground plane reduce the efficiency of the HTS antennas. Identification of these losses and their reduction are currently in progress. A complete description of this antenna, the matching network design, and full experimental results are planned for a future paper.

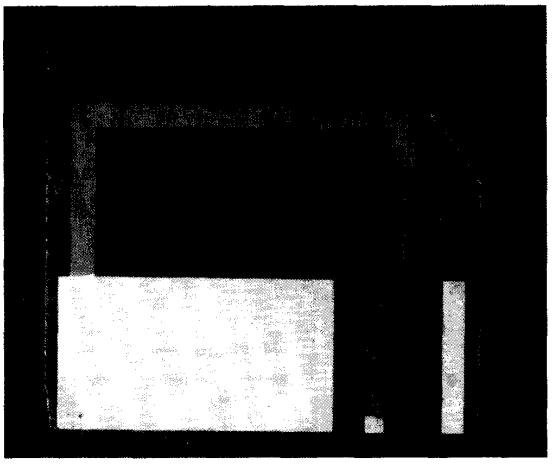

(a)

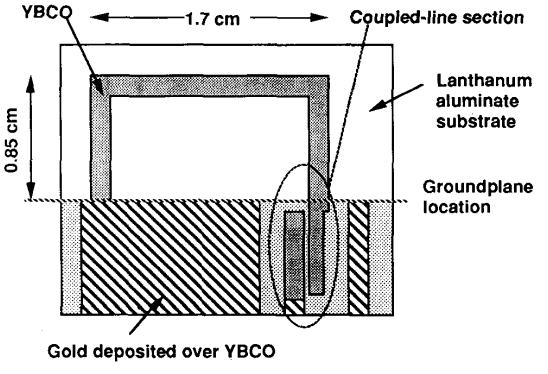

(b)

Fig. 7. (a) Thin-film YBaCuO half-loop antenna. (b) Key to photograph of antenna. The TlBaCaCuO antenna is very similar to the pictured antenna.

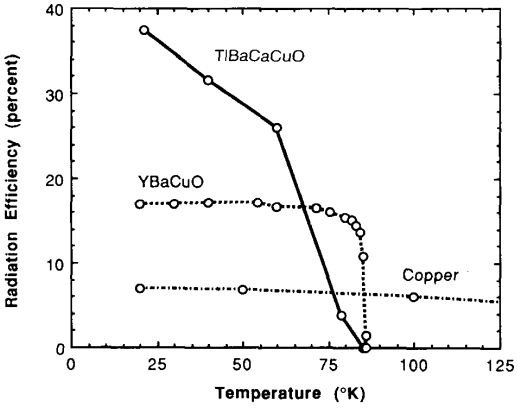

Fig. 8. Radiation efficiency measured for half-loop YBaCuO and TlBaCaCuO antennas as a function of device temperature, compared with similar measurements for a copper antenna.

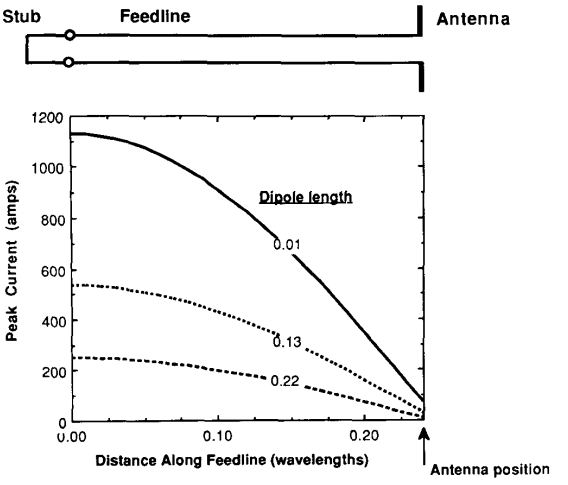

Fig. 9. Peak current in the matching network of the antenna in Fig. 2 for an input power of 1 kW.

D. Application to Transmitting Antennas

The peak currents in the matching network and on the antenna will determine the suitability of a HTS antenna for high-power transmit applications, for which current-handling capability and efficiency are both required. For the antenna of Fig. 2, we plot in Fig. 9 the current distribution on the feed line, with dipole length as a parameter. This plot emphasizes that a matching network for an electrically short antenna is essentially a near-quarter-wave transmission cavity strongly coupled at the input and weakly coupled at the output. Short antennas can produce very large currents at the input. (Actually, the maximum current occurs at the short circuit on the stub, but the value is only slightly larger than the input value because the stub is relatively short.)

Experimental investigations of the power limitations of HTS material use the value of the RF magnetic field, H_{rf}, in the transmission line as the power variable, rather than current density [9]. Fig. 10 plots the peak value of H_{rf} as a function of the peak radiated power. We selected a frequency of 100 MHz to generate this plot, since potential transmitter applications on mobile platforms exist for very short antennas in this frequency band. The results in [9] show that increases in the value of R_s begin to occur when the value of H_{rf} approaches the range of a few hundred oersteds. Fig. 10 indicates that peak radiated powers approaching 1 kW may be possible with dipoles of length 0.15λ to 0.25λ. Actually, higher radiated power levels may be feasible with coaxial transmission lines, since the closely spaced twin-lead transmission line configuration used here produces relatively large values of H_{rf} for a given current on the line. A coaxial transmission line with an inner conductor of the same diameter as one of the twin leads in our example can carry 11.5 times the current for the same value of H_{rf}.

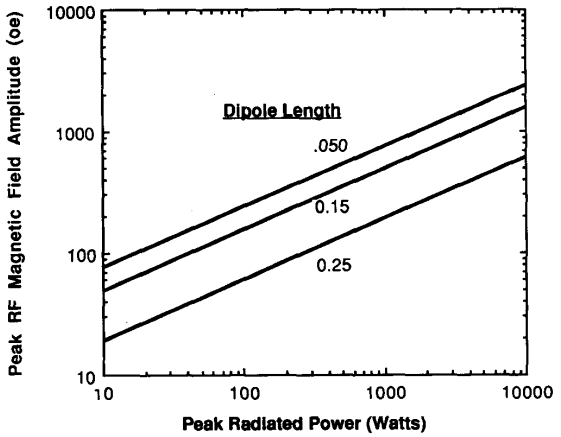

Fig. 10. Peak value of H_{rf} versus radiated power.

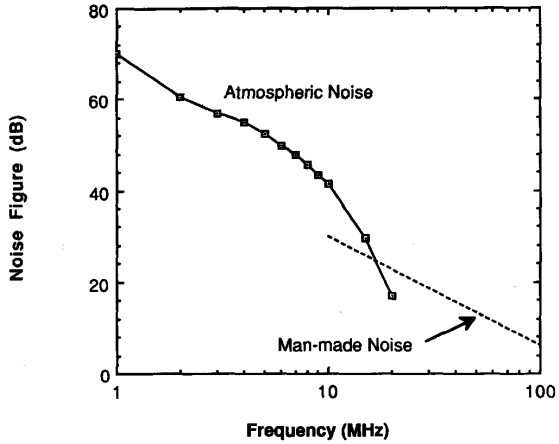

Fig. 11. Spatially averaged noise incident on a receiving antenna at a typical midlatitude site (southern England in summer).

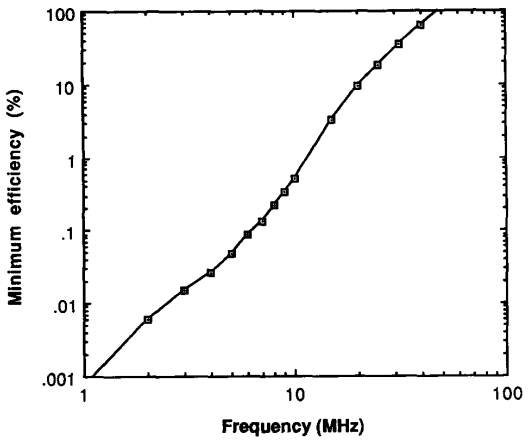

Fig. 12. Minimum antenna radiation efficiency needed to guarantee that the receiver is limited by the ambient noise of Fig. 11.

E. Applications to Receiving Antennas

For receiving applications the important quantity is the signal-to-noise ratio (SNR), rather than the antenna efficiency. The high external ambient noise below 50 MHz or so limits the usefulness of HTS antennas for reception to frequencies above this value, as shown by the following development.

Consider an antenna connected to a receiver. The system SNR can be written as [10]

$$\text{SNR} = \frac{\eta S_0(\lambda^2/4\pi)D(\theta_0,\phi_0)}{\eta\langle N_{\text{ex}}\rangle + N_a + N_R} \tag{4}$$

where S_0 is the external signal power density incident from the direction (θ_0,ϕ_0), $D(\theta,\phi)$ is the directive gain, N_a and N_R are powers at the antenna/load interface arising from internal antenna noise and receiver noise, respectively, and

$$\langle N_{\text{ex}}\rangle = (4\pi)^{-1}\int D(\theta,\phi)N_{\text{ex}}(\theta,\phi)\sin\theta\, d\theta\, d\phi$$

is the spatially averaged external noise level. If external noise dominates the internal noise and receiver noise, i.e., if

$$\eta\langle N_{\text{ex}}\rangle \gg N_a + N_R \tag{5}$$

then from (4) the SNR is independent of antenna efficiency. In this case, the use of HTS materials would not be warranted.

To determine the conditions under which the receiving system is limited by external noise, we first divide each of the noise powers in the denominator of (4) by $k_B T_0 B$ (k_B = Boltzmann's constant, $T_0 = 290$ K) so that we can compare noise figures. In Fig. 11 we plot the noise figure of typical midlatitude external noise on the surface of the earth from 1 to 100 MHz [11]. Replacing the "$\gg$" sign in (5) by a factor of 10 and setting $N_a + N_R = 10$ dB (a conservative value), we can then use Fig. 11 to determine the minimum value of η that ensures that the SNR is external-noise-limited. This minimum η is plotted in Fig. 12. This plot shows that below approximately 50 MHz the antenna can have less than 100% efficiency without affecting system SNR. The minimum efficiency curve can shift left or right a few tens of MHz if other external noise curves are used, but in general it is clear that the potential high efficiency offered by short HTS matching networks and antennas would not have an effect on system SNR below about 30 MHz.

III. Superdirective Arrays

Superdirective array excitations [12] produce a directive gain that is substantially larger than a conventional uniform or tapered excitation. Successful experimental superdirective arrays have been demonstrated (with normal metal components) [10], [13], [14], but the efficiency is low. A two-element superdirective array with high efficiency has been demonstrated using low-temperature su-

perconductors [15]. HTS materials should permit efficient superdirective arrays to be fabricated. This section briefly reviews the mathematical background and presents some calculated results of the expected improvement.

A. Maximization of the SNR

Consider a linear receiving array of equally spaced isotropic antenna elements. The normalized pattern of this array can be written as

$$F(\theta) = \sum_{n=1}^{N} W_n e^{jk(n-1)d\sin\theta} \tag{6}$$

where $W_n = A_n e^{j\theta_n}$, $k = 2\pi/\lambda$, λ is wavelength, and θ is measured relative to array broadside. By defining the weights W_n in (6) as a vector:

$$\boldsymbol{W} = [W_1 \quad W_2 \quad \cdots \quad W_n]^T \tag{7}$$

(in which the superscript T indicates the transpose) and defining the signal vector

$$\boldsymbol{S} = [1 \quad e^{jkd\sin\theta} \quad e^{j2kd\sin\theta} \quad \cdots \quad e^{jk(N-1)d\sin\theta}]^T \tag{8}$$

(6) can be written compactly as

$$F(\theta) = \boldsymbol{W}^T\boldsymbol{S}. \tag{9}$$

The array output power as a function of θ then is given by

$$P(\theta) = |\boldsymbol{W}^T\boldsymbol{S}|^2 = \boldsymbol{W}^{*T}\mathbb{P}\boldsymbol{W} \tag{10}$$

where $\mathbb{P}$ is the signal cross-spectral density matrix. For a single coherent wavefront, $\mathbb{P}$ reduces to a rank 1 dyad given by $\mathbb{P} = \boldsymbol{S}\boldsymbol{S}^*$.

The noise power at the array output of the summing device is given by

$$P_n = \boldsymbol{W}^T\mathbb{R}\boldsymbol{W} \tag{11}$$

where $\mathbb{R}$ is the noise covariance matrix, defined coefficient by coefficient as

$$\mathbb{R}_{ij} = \int n_i^*(t)n_j(t)\,dt \tag{12}$$

in which $n_i(t)$ is the noise at element i as a function of time t. Combining (10) and (11), the SNR as a function of θ is given by

$$\mathrm{SNR}(\theta) = \frac{\boldsymbol{W}^{*T}\mathbb{P}\boldsymbol{W}}{\boldsymbol{W}^{*T}\mathbb{R}\boldsymbol{W}}. \tag{13}$$

We note in passing that (4) can be derived from this equation.

We now want to find the $\boldsymbol{W}$ that maximizes SNR(θ). Equation (13) is the ratio of two bilinear forms, for which optimization techniques have been treated extensively in the literature [16]. There is a unique solution to (13) that produces the highest possible value of SNR; it is given by

$$\boldsymbol{W}_{\mathrm{opt}} = \mathbb{R}^{-1}\boldsymbol{S}_0^* \tag{14}$$

where $\boldsymbol{S}_0 = \boldsymbol{S}(\theta_0)$. Equation (14) is the solution for an *unconstrained* superdirective excitation. In practice, this excitation requires a degree of precision in specifying the feed network components and antenna elements that is nearly impossible to achieve. A constrained $\boldsymbol{W}_{\mathrm{opt}}$ solution was found in [16] by using a Lagrange multiplier ϵ to "mix" in a portion of the conventional array excitation with the unconstrained superdirective excitation. The solution for $\boldsymbol{W}_{\mathrm{opt}}$ is given by

$$\boldsymbol{W}_{\mathrm{opt}} = [\mathbb{R} + \epsilon\mathbb{I}]^{-1}\boldsymbol{S}_0^*. \tag{15}$$

This is the desired constrained superdirective solution. For $\epsilon = 0$, the unconstrained solution, (14), is recovered; as $\epsilon \to \infty$, a conventional array excitation with uniform amplitude weighting and uniform progressive phase shift results. In our notation the array Q is given by

$$Q = \frac{\boldsymbol{W}_{\mathrm{opt}}^{*T}\boldsymbol{W}_{\mathrm{opt}}}{\boldsymbol{W}_{\mathrm{opt}}^{*T}\mathbb{R}\boldsymbol{W}_{\mathrm{opt}}}. \tag{16}$$

Equations similar to these in perhaps a somewhat more familiar form can be found in [17].

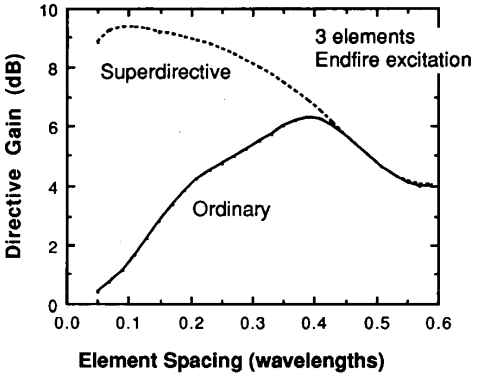

Fig. 13. Comparison of directive gain for a three-element end-fire array of isotropic elements with superdirective and ordinary excitations, as calculated from (14). The superdirective curve represents the directive gain from an unconstrained solution.

In Fig. 13 we plot a curve of the superdirective gain produced by the excitation of (14) for a three-element end-fire array and compare it with the conventional excitation. The superdirective excitation is observed to produce a directive gain that is significantly larger than an ordinary array for an element spacing less than about 0.4λ. This is the *superdirective effect*: the increase in the directive gain, when compared with the conventional uniform progressive phase shift excitation, that can be achieved when the element spacings of an array are less than about 0.4λ. Fig. 14 is a comparison of the antenna patterns for a three-element array and a six-element array.

B. Superdirective Array Properties

An intuitive understanding of the origin of the superdirective effect can be gotten from the steps shown in Fig. 15. We couch the argument in terms of a transmitting array, but the same arguments hold for a receiving array. A conventional array with 0.5λ-spaced elements is com-

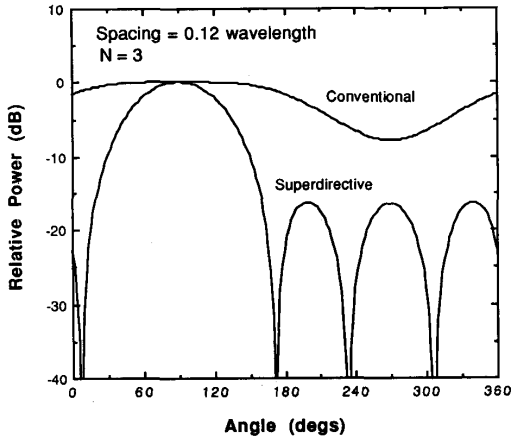

(a)

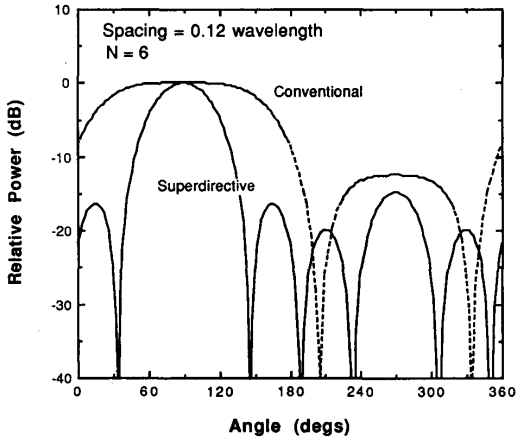

(b)

Fig. 14. Examples of antenna patterns for end-fire arrays of isotropic elements. These patterns were calculated using the constrained solution of (15) with $\epsilon = 0.002$. (a) $N = 3$ elements. (b) $N = 6$ elements.

pressed in size, and the elements are then driven with an approximate 180° progressive phase shift. This excitation tends to lead to cancellation of fields in the radiation zone and to large reactive fields in the near zone. However, some power is radiated, and by tweaking of the current phases and amplitudes (as given by (15)) this power can be made to radiate in a well-defined narrow beam.

The preceding picture helps in understanding the following summary of the properties of superdirective excitations:

1) The directive gain enhancement is most significant for end-fire arrays (that is, a beam scan angle of $\theta_0 = 90°$).
2) A point of diminishing returns is reached as the number of elements is increased beyond approximately 10. That is, superdirectivity is basically a phenomenon appropriate only for relatively small arrays.
3) Because of the antiphasal current excitation (Fig. 15), the current magnitudes necessary to generate a given power density in the far field become progressively larger as the element spacing is decreased (that is, as the array is made progressively more superdirective). For a receiving array the effect is to decrease the power delivered to the receiver. The result is low radiation efficiency.
4) The "extra" power pumped into the array because of the larger required current magnitudes is stored in reactive fields in the vicinity of the array elements. Because

$$\text{Bandwidth} = 1/Q = \frac{\text{energy dissipated per second}}{\omega\ (\text{time-average stored energy})} \tag{17}$$

where ω is the radian frequency, the large stored energy leads to a small bandwidth. We emphasize that the bandwidth of a superdirective array is narrow regardless of whether the antenna elements are electrically short or resonant. The radiation efficiency is low because large currents in the feed network and antenna elements lead to proportionally large losses.

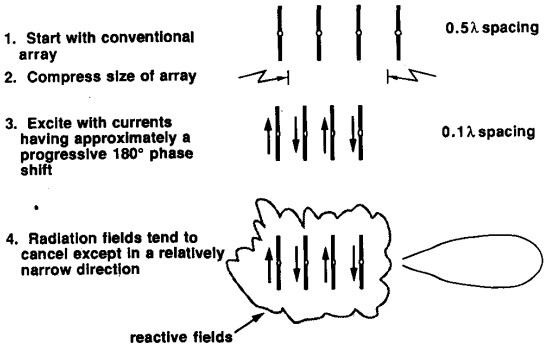

Fig. 15. Intuitive picture of the origin of superdirective excitations.

C. Superdirective Arrays and HTS's

HTS material can help in superdirective arrays of electrically small antenna elements by reducing the losses in both the feed network and the elements themselves. Fig. 16 displays the trade-off between the array Q, the beam width, and the radiation efficiency for an end-fire array of five elements separated by 0.1λ. The elements are 0.07λ long dipoles with a diameter of 0.002λ. For this calculation, the only losses are in the elements themselves; the feed network is assumed to be lossless. These curves, which were calculated using the W_{opt} of (15), were generated by varying ϵ from 0 (the rightmost points on the curves, where the excitation is the most superdirective) to

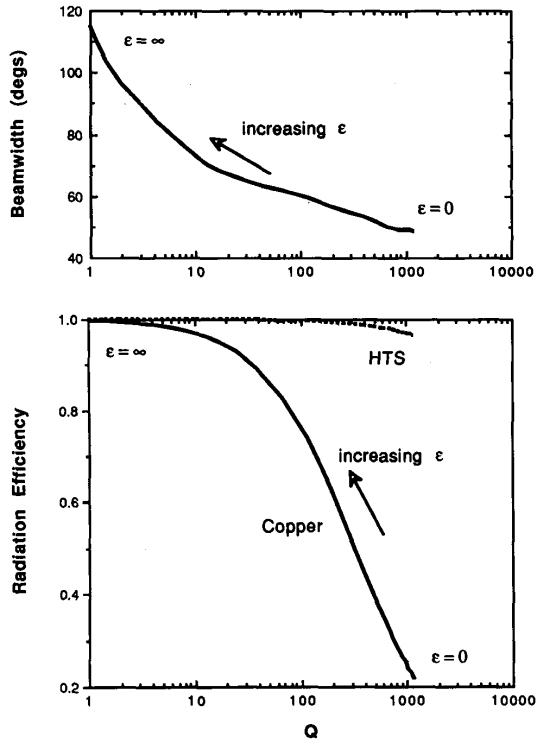

Fig. 16. Trade-off between array Q, radiation efficiency, and beam width for a five-element end-fire array with 0.1λ-element spacing. The copper curve assumes $R_s = 6.0$ mΩ (appropriate for copper at 1 GHz); the HTS curve assumes $R_s = 0.06$ mΩ.

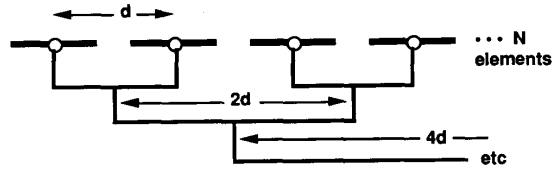

Fig. 17. Array fed by corporate network. For the purpose of calculating the feed network losses (eq. (18)), the sections of transmission line in the vertical direction are assumed to have zero length.

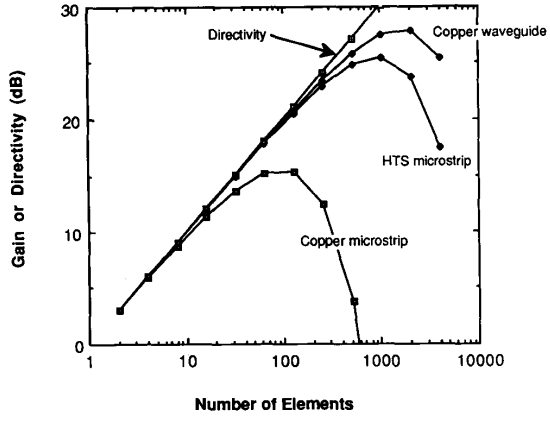

Fig. 18. Comparison of gain and directivity at 10 GHz for a corporate-fed linear array using various transmission lines in the feed network. Element spacing = 0.5λ. The HTS material is assumed to be ten times better than copper.

$\epsilon = \infty$ (the leftmost points, an ordinary end-fire excitation). Copper causes the radiation efficiency to drop precipitously, but HTS material maintains an efficiency of nearly 100%. The inclusion of losses in a feed network would further reduce the efficiency of the copper array and show an even larger relative improvement for HTS.

An important issue is the array Q that can be tolerated for a practical array. System requirements, of course, will dictate the basic necessary bandwidth, which for some applications could permit a Q approaching 1000 (a bandwidth of 500 kHz at a frequency of 500 MHz, for example). However, unavoidable variations in the near-field environment of the antenna and component tolerances may make such a high Q difficult to deal with in practice. Note that if one decides the Q must be significantly lower in a given application (100, for example), then the advantage of HTS elements is marginal. But HTS matching and feed networks for the array can offer a significant advantage for electrically small elements.

IV. Feed Networks for Millimeter-Wave Arrays

Consider the corporate feed network shown in Fig. 17. As the number of elements increases, the number of sections of transmission lines in the feed network also increases. Clearly, at some point as the array is made larger, the increased lengths of transmission lines in the feed network dissipate more power than is added to the total radiated power, so that the array gain decreases with increasing array size. The lower loss of HTS transmission lines can lead to larger arrays with higher gain.

To examine the situations in which HTS's can offer the biggest payoff for array feed networks, we use a linear array with a corporate feed network as an example. For planar arrays and other types of feed networks (such as series feeds or series/parallel combinations), the conclusions are similar.

For the array in Fig. 17, we assume the radiation efficiency of each element to be 100%. We also assume that the power is split equally at each divider, so that the array excitation is uniform. The phase gradient is zero across the array (broadside beam). For an attenuation α on the feed network transmission lines in nepers/wavelength, it can be shown that the overall efficiency of the array is given by

$$\eta = 1 - \sum_{k=1}^{j} \left\{ \left[1 - \exp\left(-2^{j-k} \alpha d \right) \right] \cdot \exp\left[2^{j} \alpha d \left(1 - \sum_{m=0}^{k-1} 2^{-m} \right) \right] \right\} \quad (18)$$

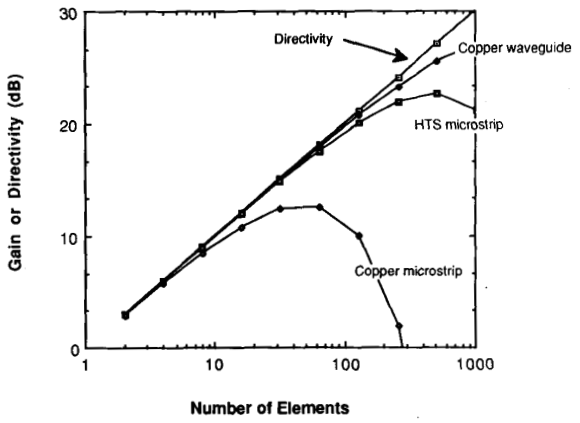

Fig. 19. Plot similar to Fig. 18 at a frequency of 35 GHz.

where d is the element separation in wavelengths, $j = \log_2 N$, and N is the total number of elements. Since the array directivity for a linear uniform array is $D = 2Nd$, the array gain is

$$G = \eta D = 2\eta Nd. \tag{19}$$

Figs. 18 and 19 are plots of (19) for attenuation values appropriate for waveguide and two microstrip transmission lines at a frequency of 10 GHz and 35 GHz, respectively. Keep in mind that these plots refer to a linear array; approximate values for a square planar array can be obtained by squaring the number of elements and multiplying the gain or directivity (in dB) by 2. Considering the 10 GHz case first, the gain peaks at about 2000 elements for copper waveguide. The much higher attenuation of copper microstrip transmission lines lowers the peak to about 100 elements, which is increased to 1000 elements if the microstrip transmission line is fabricated from HTS material. For 35 GHz, the situation is much the same, except that the peak for copper microstrip is even lower, at about 50 elements. Clearly, HTS microstrip feed networks can lead to larger arrays with higher gains compared with copper microstrip.

However, HTS is likely to find an application only at 35 GHz (and higher frequencies) because of 1) the tolerances, cost, and general difficulty of using waveguide at this frequency and 2) the smaller physical size of an array of a given number of elements. At 10 GHz very large waveguide-fed slot arrays can be easily fabricated; there appears to be little benefit in replacing relatively low loss copper waveguide with HTS microstrip. In addition, the physical size of a 10 GHz array of hundreds of elements (4.5 m for a 300 element linear array with half-wavelength spacing) would pose a formidable cooling problem. On the other hand, a 100 element array at 35 GHz, which would benefit substantially by a HTS microstrip feed network, is 43 cm long, a size for which cooling could be provided without substantial difficulty.

V. Signal Processing Arrays

Finally, we mention the possibility of integrating passive signal processing elements into the feed network to form a system that sorts signals in the time, frequency, and spatial domains in one passive network. The very low insertion loss (0.1 dB and less) demonstrated [18] for delay lines and filters would permit them to follow immediately behind the receiving elements, without any intervening amplifiers. One can conceive of very broad band arrays using delay lines for beam steering. Large filter banks could be incorporated ahead of the first stage of amplification. If HTS films can be shown to have a useful infrared response, there is also the possibility of an integrated RF and infrared sensor/antenna.

VI. Practical Considerations

Providing cryogenic cooling for antennas, matching networks, and array feed networks presents some unique challenges not encountered in other potential RF and microwave applications of HTS's. Antennas, by their very nature, are open structures for which it is desirable to keep all nonmetallic materials and all non-HTS metallic parts as small and as far away as possible. Essentially all successful (low-temperature) superconducting antennas used to date [1] have operated in the frequency band from 0.3 Hz to 300 Hz, where the wavelength is so long that interactions with nearby materials are not a serious problem and where conventional nonmetallic Dewars are sufficiently transparent. In the frequency range from 1 MHz to 100 GHz, the cooling shrouds, radiation baffles, insulation, and cryogens associated with cryogenic cooling will interfere with the radiation pattern and efficiency.

Cooling only the matching network is clearly somewhat less daunting than cooling the radiating elements, but requires careful design. It is necessary to impedance match the antenna side of the network directly to the antenna and to keep the transmission line between matching network and antenna as short as possible; this presents a heat conduction problem. Noncontact capacitive coupling would help in this regard.

Cooling an entire feed network for an array seems to be feasible only if the size of the array can be kept reasonably small, on the order of a few tens of centimeters. For this reason millimeter-wave arrays may be a good application, even though the improvement of HTS material over copper decreases as the frequency is increased. As mentioned above, compact superdirective arrays from 100 MHz to 1 GHz can profitably make use of the low loss of HTS material and keep within such a size constraint.

VII. Conclusions

We have shown that an increase in efficiency is possible for electrically short antennas, but at the expense of bandwidth. In most practical applications to ground-based, shipboard, airborne, and space-borne antennas, resonant antennas can be used above several GHz. Hence, systems

operating below about 3 GHz are the prime candidates for electrically short HTS antennas. Substantial radiated power levels (on the order of kilowatts) can be handled by the best HTS material. For receiving applications subjected to terrestrial noise, the improvement in efficiency is only beneficial above a frequency of 30 MHz or so. Substantial (and sufficient) improvement may be realized by making only the matching network of HTS material. The losses in accompanying dielectric materials must be kept low (loss tangents less than 10^{-4}). Preliminary experimental results have shown an increase in efficiency from 7% to 37% for a half-loop TlBaCaCuO antenna, relative to copper.

HTS material should permit enhanced-gain superdirective arrays to be fabricated that have high efficiency. As with single elements, the frequency band of application is below 3 GHz. Most applications above this frequency can accommodate arrays large enough so that that superdirective excitations are not needed.

Millimeter-wave arrays should benefit from HTS material, even though the improvement of R_s over copper is less than at lower frequencies, because the feed network losses are very sensitive to the value of R_s. It has been suggested [19] that the biggest payoff may occur at frequencies above 100 GHz if microstrip lines with very thin dielectric spacings (100 μm or less) can be fabricated.

Acknowledgment

The authors express their gratitude to J. Talvacchio of the Westinghouse Science and Technology Center in Pittsburgh, PA, for providing the patterned Y-Ba-Cu-O film and to V. Hietala of Sandia National Laboratory for providing the patterned TlBaCaCuO film.

References

[1] J. R. Davis, R. J. Dinger, and J. Goldstein, "Development of a superconducting ELF receiving antenna," *IEEE Trans. Antennas Propagat.*, vol. AP-25, pp. 223–231, 1977.
[2] R. C. Hansen, "Superconducting antennas," *IEEE Trans. Aerosp. Electron. Syst.*, vol. 26, no. 2, pp. 345–355, 1990.
[3] J. T. Williams and S. A. Long, *Antennas and Propagation Magazine*, vol. 32, no. 4, pp. 7–12, 1990.
[4] R. J. Dinger, "Some potential antenna applications of high-temperature superconductors," *J. Superconductivity*, vol. 3, no. 3, pp. 287–296, 1990.
[5] W. L. Stutzman and G. A. Thiele, *Antenna Theory and Design*. New York: Wiley, 1981.
[6] H. A. Wheeler, "Fundamental limitations of small antennas," *Proc. IRE*, vol. 35, pp. 1479–1484, 1947.
[7] S. K. Khamas *et al.*, "A high-T_c superconducting short dipole antenna," *Electron. Lett.*, vol. 24, pp. 460–461, 1988.
[8] R. J. Dinger and D. J. White, "Theoretical increase in radiation efficiency of a small dipole antenna made from high temperature superconductors," *IEEE Trans. Antennas Propagat.*, vol. 38, pp. 1313–1316, 1990.
[9] C. L. Bohn, J. R. Delayen, D. I. Dos Santos, M. T. Lanagan, and K. W. Shepard, *IEEE Trans. Magn.*, vol. 25, no. 2, pp. 2406–2409, 1989.
[10] E. H. Newman, J. H. Richmond, and C. H. Walter, "Superdirective receiving arrays," *IEEE Trans. Antennas Propagat.*, vol. AP-26, pp. 629–635, 1978.
[11] E. N. Skomal, *Man-Made Radio Noise*. New York: Van Nostrand, 1978.
[12] S. A. Schelkunoff, "A mathematical theory of linear arrays," *Bell Syst. Tech. J.*, vol. 2, no. 1, 1943.
[13] A. Bloch, R. G. Medhurst, and S. D. Pool, "A new approach to the design of super-directive aerial arrays," *Proc. Inst. Elec. Eng.*, pt. III, vol. 100, pp. 303–314, 1953.
[14] E. H. Newman and M. R. Schrote, "A wide-band electrically small superdirective array," *IEEE Trans. Antennas Propagat.*, vol. AP-30, pp. 1172–1176, 1982.
[15] G. B. Walker, C. R. Haden, and O. G. Ramer, "Superconducting superdirectional antenna arrays," *IEEE Trans. Antennas Propagat.*, vol. AP-25, pp. 885–887, 1977.
[16] H. Cox, R. M. Zeskind, and T. Kooij, "Practical supergain," *IEEE Trans. Acoust., Speech, Signal Process.*, vol. ASSP-34, pp. 393–398, 1986.
[17] D. K. Cheng and F. I. Tseng, "Gain optimization for arbitrary antenna arrays," *IEEE Trans. Antennas Propagat.*, vol. AP-13, pp. 973–974, 1965.
[18] J. Bybokas and R. Hammond, *Microwave J.*, vol. 33, p. 127, 1990.
[19] E. B. Ekholm and S. W. McKnight, "Attenuation and dispersion for high-T_c superconducting microstrip lines," *IEEE Trans. Microwave Theory Tech.*, vol. 38, pp. 387–395, 1990.

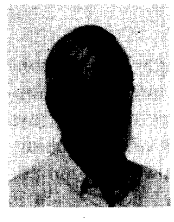

Robert J. Dinger (M'90) was born in Washington, DC, on August 7, 1943. He received the Ph.D. degree in physics from the University of California, Riverside, in 1971.

Upon graduation, he joined the Research Department at the Naval Weapons Center (NWC), China Lake, CA, working in the area of millimeter-wave nonreciprocal devices and superconducting magnetometers. In 1974, he accepted a position with the Naval Research Laboratory (NRL), Washington, DC, in the Communication Sciences Division. From 1974 to 1981, he conducted research at NRL successively in the areas of cryogenic receivers for ELF submarine communications, noise and propagation in the lower VLF band, the spatial coherence of atmospheric noise in the ULF and ELF bands, and compact high-frequency adaptive arrays. In 1981, he returned to NWC as the head of the RF and Microwave Technology Branch in the Research Department. His current interests include adaptive array processing, radar glint measurements, radar imaging, superdirective arrays, and microwave applications of high-temperature superconductivity.

Donald R. Bowling was born in Covington, KY, on August 20, 1949. He received the B.S. and M.S. degrees in electrical engineering from Michigan State University in 1971 and 1972 respectively.

Since then he has been employed at the Naval Weapons Center, China Lake, CA, where in 1987 he became a member of the RF and Microwave Technology Branch in the Research Department. His current research interests include millimeter-wave solid-state power combining and high-temperature-superconductor antenna design.

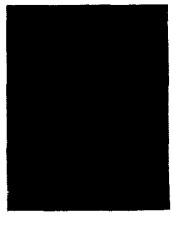

Anna M. Martin received the B.S. degree in physics from the University of California, Los Angeles, in 1988. Her interests at UCLA were plasma physics and astronomy.

Since 1988, she has been a Research Physicist at the Naval Weapons Center, China Lake, CA, where she has been measuring the dc and RF properties of high-temperature superconductors.